# Thermodynamics of DNA−RNA Heteroduplex Formation: Effects of Locked Nucleic Acid Nucleotides Incorporated into the DNA Strand†

Harleen Kaur,‡ Jesper Wengel,§ and Souvik Maiti*,‡

*Institute of Genomics and Integrative Biology, CSIR, Mall Road, Delhi 110 007, India, and Nucleic Acid Center, Department of Chemistry, University of Southern Denmark, DK-5230 Odense M, Denmark*

*Received May 23, 2007; Revised Manuscript Received October 16, 2007*

ABSTRACT: A locked nucleic acid (LNA) monomer is a conformationally restricted nucleotide analogue exhibiting enhanced hybridization efficiency toward complementary strand. The potential of LNA-based oligonucleotides has been sought to improve the selectivity and specificity of probe sets employed in detection and specific targeting of nucleic acids. We have evaluated the influence of "locked nucleic acid" residues on hybridization thermodynamics, counterions and hydration of DNA·RNA heteroduplex using spectroscopic and calorimetric techniques. One to three LNA substitutions have been introduced either at the adenine (5′-AGCACCAG) or thymine (5′-TGCTCCTG) residues of the DNA strand. A complete thermodynamic profile for heteroduplex formation suggested that LNA-induced stabilization results from a favorable increase in the enthalpy of hybridization that compensates for the unfavorable entropy change. Analysis of differential scanning calorimetry data indicated a nonzero heat capacity change, $\Delta C_p$, accompanying the heteroduplex formation. Isothermal titration calorimetry measurements indicated an increase in binding affinity of the two strands as the LNA content of the heteroduplex is increased. Overall our result demonstrated that the effect of LNA-substitution at the thymine residue is more pronounced compared to the adenine residue. Furthermore, optical melting studies showed that, compared to an unmodified duplex, the formation of LNA-modified duplex is accompanied by a higher uptake of counterions and a lower uptake of water molecules. Our result, thus, presents a preliminary attempt toward the characterization of hybridization thermodynamics of the LNA-based probe-target sets, which will in turn aid in the selection of optimal conditions for hybridization experiments, and evaluation of the minimum probe-length required for hybridization and cloning experiments.

Specific targeting and inactivation of gene expression by oligonucleotide-based therapeutics is a promising alternative to the conventional therapeutic strategies. The last two decades have seen an upsurge in the synthesis of modified nucleotide analogues with desirable therapeutic properties and commercial viability (*1*). A locked nucleic acid (LNA) is one such engineered nucleic acid analogue, containing one or more LNA nucleotide monomers with a bicyclic furanose unit locked in an RNA-mimicking sugar conformation (Scheme 1) (*2*). This conformational restriction results in a locked 3′-endo conformation that is translated into unprecedented hybridization affinity toward complementary DNA/RNA without loss of specificity, which makes fully modified LNAs, LNA/DNA mixmers, or LNA/RNA mixmers uniquely suited for mimicking and targeting nucleic acid secondary structures *in vitro* or *in vivo* (*3*−*5*). With regard to antisense therapy, the superior specificity of LNA probes allows selective targeting of even short-length, minority miRNAs and siRNAs against a large background of cellular RNAs. Its exceptionally high specificity can be exploited to target

Scheme 1[a]

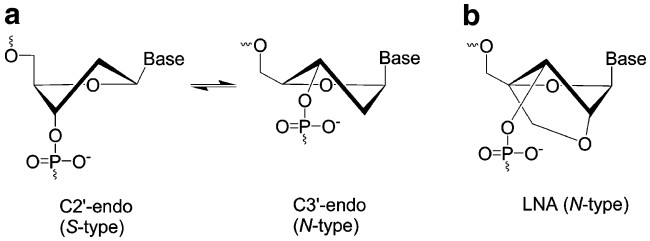


[a] (a) The C2′-endo−C3′-endo sugar ring equilibrium present in nucleic acids. (b) The molecular structure of locked nucleic acid (LNA), which shows the locked C3′-endo sugar conformation.

the highly structured RNAs that are usually inaccessible to the conventionally used unmodified DNA oligonucleotides (*6*−*13*). Furthermore, presence of an LNA-substitution enhances the metabolic stability, and improves the pharmacokinetic and the toxicity profile of the modified oligonucleotide (*9*, *14*).

The antisense efficacy of LNA-modified DNA oligonucleotides has been successfully employed in cancer therapy (*8*, *11*, *15*−*17*); for inhibiting replication of hepatitis and HIV mRNA (*18*−*21*); for understanding molecular mechanisms of various biological processes (*22*, *23*); for inhibiting the intron splicing of group 1 introns in *Candida albicans* (*11*), and as RNA capture probes for *in situ* detection of mRNA (*24*). A major breakthrough in the field of LNA-technology

† This work was supported by Council of Scientific and Industrial Research, India (Structure−function relation of modified nucleic acids).

* To whom correspondence should be addressed. Phone: +91-11-2766-6156. Fax: +91-11-2766-7471. E-mail: souvik@igib.res.in.

‡ Institute of Genomics and Integrative Biology.

§ University of Southern Denmark.

10.1021/bi700996z CCC: $40.75 
Published on Web 01/03/2008

has been its use in *in situ* detection and expression profiling miRNAs, along with their functional characterization (*25*−*31*). The aforementioned assays largely rely on specific hybridization of LNA/DNA probes to the target RNA, against a large cellular background. Consequently, accurate designing of LNA/DNA probe sets allowing for precise detection target RNAs becomes a prerequisite. In practice, the biophysical properties of LNA can be exploited to design a probe set to ensure uniform, high-affinity hybridization yielding highly accurate signals that could discriminate even single nucleotide differences and closely related RNA family members. Our study represents a preliminary step in realization of creating a probe dataset based on thermodynamics characterization of LNA/DNA·RNA heteroduplex hybridization. Starting with short oligonucleotide sequences containing varying amounts of LNA-substitution, we have evaluated the influence of LNA-modification on hybridization thermodynamics, counterion changes and hydration of DNA·RNA heteroduplex.

The hybridization properties of LNA containing oligonucleotides have been evaluated in different sequence context ranging from six to twenty nucleotide long oligomers with varying LNA content and architecture (such as fully modified LNA, LNA/DNA mixmers, LNA/RNA mixmers, LNA/PS-DNA mixmers) (*3*, *32*, *33*). Substitution by an LNA monomer leads to a rise in the $\Delta T_m$ values up to +1 to +8 °C against DNA and an increase of +2 to +10 °C against RNA (*10*, *12*, *32*−*34*). This is possibly the largest increase in thermostability observed for a nucleic acid analogue, which nevertheless saturates when the relative substitution by LNA monomer reaches to about 50% of the total residues in the LNA/DNA chimera (*34*−*36*). Further, the impact on the thermostability depends on the oligomer length and composition. A few reports based on thermodynamic evaluation of LNA-mediated nucleic acid hybridization showed that the introduction of an LNA modification induces entropically favored duplex formation, compared to the unmodified duplexes, while duplex formation for the all-modified LNA appeared to be entropically disfavored and strongly enthalpically favored (*5*). Another study revealed a large positive $\Delta\Delta S$ and a negligible $\Delta\Delta H$ for a gapmer with seven LNAs (*36*). A hybridization kinetics study using stopped-flow kinetics has also been performed. Evaluation of thermodynamics for the same oligonucleotides showed small negative $\Delta\Delta H$ and $\Delta\Delta S$ values for LNA-modified duplex formation (*37*). Another study examined the sequence-dependent effects of LNA on hybridization thermodynamics and observed it to be largely influenced by the neighboring bases flanking the substitution (*38*). The effects of LNA substitutions as a function of sequence context in the middle of the 2′-*O*-methyl substituted RNA heptamer have also been investigated and found to be approximately additive when LNA nucleotides are separated by at least one 2′-*O*-methyl nucleotide (*39*). The studies mentioned above represent a preliminary evaluation of LNA-based hybridization thermodynamics, based on simple UV melting experiments.

In an attempt to study the origin of enhanced-stability for LNA residues, we analyzed hybridization thermodynamics of LNA-based oligonucleotides in different model systems. In our earlier work (*40*) we employed both spectroscopic and calorimetric measurements to investigate the effect of LNA on hybridization thermodynamics of DNA duplex formation. Using the same sequence sets we now evaluate the energetics, counterion and hydration effects accompanying the formation of 8-mer LNA-modified RNA·DNA (RNA·LNA/DNA) hetroduplex. For all the modified oligonucleotides (8-mer), substitutions were introduced at adenine or thymine nucleotides of the DNA strand of the heteroduplex. Our ITC and DSC data for the heteroduplex formation indicates that increase in LNA substitution leads to an increase in enthalpy change which compensates for the unfavorable entropy change, thereby making the overall process of duplex formation energetically more favorable than unmodified duplex. The heat capacity change, $\Delta C_p$, accompanying each heteroduplex formation, obtained through DSC, has also been reported and has been used to furnish thermodynamic parmeters at 37 °C. Our ITC data shows an increase in the binding constant ($K_a$) of the two strands concomitant with the increase in extent of LNA substitution. Further, the formation of the LNA-modified hetroduplex is associated with the higher uptake of sodium ions and lower uptake of water molecules with respect to the unmodified DNA·RNA hetroduplex.

Table 1: Heteroduplexes Containing LNA Modifications in Boldface with L Superscript

| nomenclature | sequence (8-mer) | nomenclature | sequence (8-mer) |
|---|---|---|---|
| T-LNA0 | 5′-TGCTCCTG-3′<br>3′-ACGAGGAC-5′ | A-LNA0 | 5′-AGCACCAG-3′<br>3′-UCGUGGUC-5′ |
| T-LNA1 | 5′-**T**$^{L}$GCTCCTG-3′<br>3′-ACGAGGAC-5′ | A-LNA1 | 5′-**A**$^{L}$GCACCAG-3′<br>3′-UCGUGGUC-5′ |
| T-LNA2 | 5′-**T**$^{L}$GC**T**$^{L}$CCTG-3′<br>3′-ACGAGGAC-5′ | A-LNA2 | 5′-**A**$^{L}$GC**A**$^{L}$CCAG-3′<br>3′-UCGUGGUC-5′ |
| T-LNA3 | 5′-**T**$^{L}$GC**T**$^{L}$CC**T**$^{L}$G-3′<br>3′-ACGAGGAC-5′ | A-LNA3 | 5′-**A**$^{L}$GC**A**$^{L}$CC**A**$^{L}$G-3′<br>3′-UCGUGGUC-5′ |

## MATERIALS AND METHODS

Two sets of 8-mer oligonucleotides were considered to study the effect of LNA on hybridization thermodynamics of DNA·RNA heteroduplex. The DNA counterpart of the heteroduplex was modified to various extents and at various positions with either adenine- or thymine-locked nucleic acid nucleotides. For each of the A- and T-modified sets, four oligonucleotide sequences, containing LNA substitutions ranging from zero to three modified nucleotides, were studied (Table 1).

All the LNA-containing octamers were synthesized and purified as described in the literature (*35*). The other unmodified oligonucleotides (HPLC-purified) were purchased from Sigma Genosys. The solution concentrations of each of the unmodified oligonucleotide were determined optically at 260 nm and 25 °C using the following molar extinction coefficients (per $mM^{-1}$ $cm^{-1}$ of strands): 81.3 for d(AGCACCAG), 64.9 for r(CUGGTUGUT), 65.7 for d(TGCTCCTG), and 83.7 for r(CAGGAGCA). These values were calculated by extrapolation of the tabulated values of the dimer and monomer nucleotides at 25 °C to high temperatures using protocols reported previously (*41*). For the modified oligonucleotides, the molar absorptivities were assumed to be identical to the DNA oligonucleotides.

All measurements were performed in 10 mM sodium cacodylate buffer (pH 7). The heteroduplex solutions were prepared by mixing the given template strand, bearing

varying amounts of LNA modifications, with the corresponding unmodified complementary strand in a 1:1 ratio. Prior to the experiments, the samples were heated to 95 °C for 20 min and then slowly annealed to the starting temperature of the experimental conditions. All experiments except DSC were performed in replicas of three with the experimental error stated as footnotes to tables.

*Temperature-Dependent UV Spectroscopy (UV Melts*). Thermal denaturation scans for each 8 bp heteroduplex were obtained with a thermoelectrically controlled Cary 100 (Varian) spectrophotometer, as a function of salt (10−110 mM $Na^+$) and osmolyte [5−25% (w/v) ethylene glycol] concentration. All melting curves for duplex denaturation were collected at a 260 nm wavelength as a function of temperature in the temperature range from 10 to 90 °C at a heating rate of 1 °C/min. The melting curves for each heteroduplex were recorded in reversible conditions. Heating−cooling cycles were performed to check if there is any hysteresis (Supporting Information Figure SI1). The mole fraction of the folded heteroduplex (α) at different temperatures was evaluated from the absorbance, and $\Delta A/\Delta A_{max}$, where $\Delta A$ is the change in absorbance at 260 nm at any temperature and $\Delta A_{max}$ is the maximum change recorded at the highest temperature, was also calculated. The plot of mole fraction (α) versus temperature allowed us to measure the melting temperature, $T_m$. Some of the original plots (abs vs temperature) are provided in Supporting Information (Supporting Information Figure SI2 and Figure SI3).

The van't Hoff enthalpy change ($\Delta H_{vH}$) for duplex formation was calculated by fitting the shape of each curve to the following equation using the MeltWin 3.5 program (*42*) that is available at www.meltwin.com,

$$\epsilon(T) = (M_{ss}T + B_{ss})\alpha + (M_{ds}T + B_{ds})(1 - \alpha) \quad (1)$$

Here, $\epsilon(T)$ represents for the temperature dependence of the extinction coefficient, $\epsilon$; the first term of the right expression indicates the mole-fraction weighted, linear component of the melt curve due to single strands, while the second term represents the mole-fraction weighted, linear component due to double strands.

The entropy and enthalpy values are calculated using the method of Gralla and Crothers (1973) according to which

$$\Delta H^\circ = C/(1/T_{1/2} - 1/T_{3/4}) \quad (2)$$

$$\Delta S^\circ = (\Delta H^\circ/T_m) + X \quad (3)$$

where $C$ is the constant 4.4, 7.0, or 3.2 cal/(mol·K) and $X$ is $\ln(C_T)$, $\ln(C_T/4)$, or 0 for self-complementary, non-self-complementary, or unimolecular equilibria, respectively; $T_{1/2}$ and $T_{3/4}$ are the absolute temperatures at the maximum and upper half-maximum of the melt curve derivative, respectively. In addition to the MeltWin program, all the melting curves were also treated manually to extract $\Delta H_{vH}$. The linear lower and upper baselines were manually chosen in the absorbance vs temperature curves and $\Delta H_{vH}$ values calculated as previously described (*43*). As the determinations of baselines are mainly biased, both of the methods have certain uncertainty. To achieve the values of best accuracy, all experiments were performed at least thrice, and several different upper and lower baselines were chosen to calculate $\Delta H_{vH}$ and the reported values are averaged values obtained from different replicas. Values found to be in agreement by both of the methods were considered to be the final ones.

Furthermore, the thermodynamic uptake of counterions, $\Delta n_{Na^+}$, associated with the process of duplex formation can be obtained according to the equation

$$\Delta n_{Na^+} = 1.11(\Delta H/RT_m^2)\, \delta T_m/\delta(\ln [Na^+]) \quad (4)$$

where 1.11 is a proportionality constant for converting ionic activity into concentrations and $\delta T_m/\delta(\ln [Na^+])$ represents the slope of a plot of $T_m$ versus the logarithm of sodium ions ($\ln [Na^+]$) at different concentrations (10−110 mM $Na^+$) (*44*). The term in parentheses is a constant obtained from the UV experiment, and $R$ represents the universal gas constant (1.986 cal $mol^{-1}$ $K^{-1}$). Similarly, the changes in the number of water molecules associated with the melting process, $\Delta n_W$, were obtained from the dependence of $T_m$ on water activity ($a_W$) according to the equation

$$\Delta n_W = (-\Delta H/R)[\delta(T_m^{-1})/\delta(\ln a_W)] \quad (5)$$

where $\Delta H$ is the enthalpy change determined from UV experiments and $R$ is the universal gas constant (*45*). The slope of the plot of reciprocal temperature ($K^{-1}$) of melting versus the logarithm of water activity ($\ln a_W$) at different concentrations (0, 5, 10, 15, 20, and 25%) of ethylene glycol gave the value of $\delta(T_m^{-1})/\delta(\ln a_W)$.

*Differential Scanning Calorimetry (DSC Melts*). Differential scanning calorimetry was used to monitor the heat capacities of each heteroduplex (30 $\mu$M) as a function of temperature (melting curves) using a VP-DSC differential scanning calorimeter (Microcal, Inc., Northampton, MA). A typical experiment consists of heating of a sample cell containing 0.52 mL of heteroduplex solution and a reference cell filled with the same volume of buffer, in the temperature range 10 to 90 °C at a rate of 1 °C/min. Repeated buffer versus buffer scans were carried out with 10 mM sodium cacodylate to obtain an appropriate, reproducible baseline which was then subtracted from the sample versus buffer scan. The average sample scans were normalized for concentration, and the progressive baseline mode available in the analysis package (Origin 7. 5) was used to integrate the resulting curve, $\int \Delta C_p\, dT$, to yield the molar unfolding enthalpy, $\Delta H_m$, near the melting temperature. $T_m$ was determined by the midpoint of the transition, while the heat capacity change, $\Delta C_p$, accompanying duplex melting was determined by the difference in between pre- and postdenaturation baseline extrapolated to the midpoint of the transition (*46*). The obtained $\Delta C_p$ values were then used to furnish a complete thermodynamic profile at 37 °C, using the following equation (*47*):

$$\Delta H(T) = \Delta H_m + \Delta C_p(T - T_m) \quad (6)$$

$$T\Delta S(T) = \Delta H_m(T/T_m) + \Delta C_p T \ln(T/T_m) \quad (7)$$

$$\Delta G(T) = \Delta H_m[(1 - T/T_m) + \Delta C_p(T - T_m) - \ln(T/T_m)] \quad (8)$$

where $T = 37$ °C and $\Delta H_m$ represents the enthalpy change around melting temperature. Furthermore, the effects of LNA incorporation on the thermodynamic parameters can be represented as the difference in the $\Delta H$ and $\Delta S$ for

hybridization between the LNA-containing heteroduplex and the unmodified heteroduplex ($\Delta\Delta H = \Delta H_{LNA+DNA:RNA} - \Delta H_{DNA:RNA}$ and $\Delta\Delta S = \Delta S_{LNA+DNA:RNA} - \Delta S_{DNA:RNA}$).

*Isothermal Titration Calorimetry (ITC).* The measurement of the heat for mixing a single RNA strand with its complementary DNA strand was carried out with the Microcal VP-titration calorimeter at 10 °C; at this temperature each duplex forms completely. For accurate estimation of $\Delta H$ values, the DNA strand with concentration 30 $\mu$M for T-LNA and 15 $\mu$M for A-LNA was loaded into a 1.4 mL sample cell, and the complementary RNA strand (titrant) at concentration 300 $\mu$M for T-LNA and 150 $\mu$M for A-LNA was loaded into the 250 $\mu$L injection syringe at the stirring rate of 400 rpm. A typical titration consisted of 10 $\mu$L injections, with 300 s interval between subsequent injections.

The resultant titration plot was fitted to a sigmoidal curve by a nonlinear least-squares method using Origin 7.0 (Microcal Software). The binding constant $K_a$, the stoichiometry $N$, and the enthalpy change $\Delta H$ were obtained from the curve fitting. The Gibbs free energy change $\Delta G$ and the entropy $\Delta S$ were calculated from the equation

$$\Delta G = -RT \ln K_a = \Delta H - T\Delta S \qquad (48, 49) \quad (9)$$

## RESULTS

*UV Melting Study*. Accurate thermodynamic parameters can be obtained from melting curves only when they exhibit the nature of true equilibrium curves, i.e., superimposable heating and annealing profiles. Under the buffer conditions and heating/cooling rate 1 °C min$^{-1}$ all eight oligonucleotides displayed superimposable and reproducible (Supporting Information Figure SI1) heating and annealing profiles. Thus, all melting curves were true equilibrium curves and were treated to extract complete thermodynamic parameters.

LNA modified-oligonucleotide substitutions are known to display enhanced thermal stability when hybridized to complementary DNA or RNA (*2*−*5*). Our optical melting data supported this finding, as for both the A- and T-modified sets, we observed significantly higher $T_m$ values relative to the unmodified heteroduplexes (Figure 1). The increment in $T_m$ per modification for A-LNA was found to be 1.0 (A-LNA1), 4 (A-LNA2), and 5 °C (A-LNA3) whereas increase of 6.0 (T-LNA1), 8.03 (T-LNA2) and 6.8 °C (T-LNA3) were recorded for T-LNA duplexes at 10 mM $Na^+$. A much prominent enhancement in $T_m$ was obtained at a higher salt concentration of 110 mM $Na^+$, where a higher $T_m$ increment per modification was detected for both the A-LNA and T-LNA duplexes (Table 2). In each case, the enhancement in the $T_m$ was much higher for T-LNA modification than for A-LNA modification. The data in Table 2 also gives the van't Hoff enthalpy change ($\Delta H_{vH}$) for each heteroduplex formation around the melting temperature, which tends to increase with increase in LNA content of the heteroduplex.

*DSC Melting Study*. Differential scanning calorimetery was used to investigate the effects of LNA incorporation on the energetics of heteroduplex-unfolding (*50*), as represented in Figure 2. An essentially flat baseline was observed for the pre- and postdenaturation region of the DSC curve. Our UV melting data also shows a similar feature, suggesting that these heteroduplexes unfold in a two state process. Furthermore, duplex melting was observed to be accompanied by a

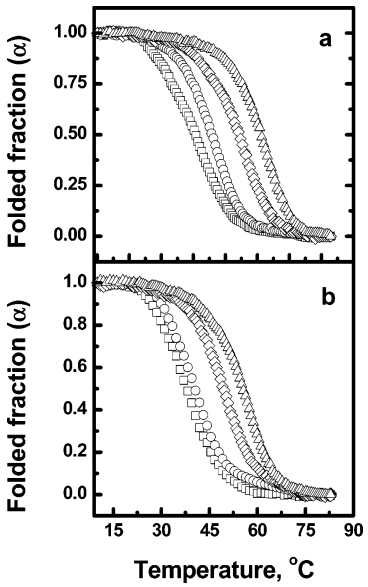


FIGURE 1: UV melting curves of unmodified (□), single (○), double (◇) and triple (△) modified heteroduplexes in 10 mM sodium cacodylate buffer with 100 mM NaCl: (a) T-LNA and (b) A-LNA.

Table 2: Melting Temperatures ($T_m$ Values) at Two Different Salt Concentrations and van't Hoff Enthalpy ($\Delta H_{vH}$) Changes at $T_m$ for Helix−Coil Transition[a]

| | $T_m$ °C | | | | |
|---|---|---|---|---|---|
| duplex | 10 mM $Na^+$ | $T_m$ enhancement per modification | 110 mM $Na^+$ | $T_m$ enhancement per modification | $\Delta H_{vH}$ (kcal/mol)[a] |
| T-LNA0 | 29.7 | | 38.6 | | −61.6 |
| T-LNA1 | 35.7 | 6.0 | 45.3 | 6.7 | −64.7 |
| T-LNA2 | 45.7 | 8.0 | 55.0 | 8.2 | −70.2 |
| T-LNA3 | 50.1 | 6.8 | 61.5 | 7.6 | −73.3 |
| A-LNA0 | 30.0 | | 39.0 | | −64.1 |
| A-LNA1 | 31.0 | 1.0 | 41.2 | 2.2 | −66.0 |
| A-LNA2 | 38.0 | 4.0 | 48.7 | 4.8 | −68.6 |
| A-LNA3 | 45.0 | 5.0 | 55.9 | 5.6 | −72.3 |

[a] All the parameters were obtained from UV experiments. Heteroduplex concentrations were 2 $\mu$M. Experiments were conducted in 10 mM sodium cacodylate buffer (pH 7.0) or 10 mM sodium cacodylate containing 100 mM NaCl. The $T_m$ values are within ±0.5 °C error while the $\Delta H_{vH}$ values are within 10% error.

nonzero heat capacity change, $\Delta C_p$, determined by the difference in between pre- and postdenaturation baseline extrapolated to the midpoint of the transition (Figure 2) (*50*,*51*). The values obtained for $\Delta C_p$ change accompanying duplex formation have been tabulated in Table 3. The average $\Delta C_p$ change observed per duplex was found to be 175 cal mol$^{-1}$ K$^{-1}$, yielding an averaged base pair change of 22 cal (mol of base pairs)$^{-1}$ K$^{-1}$. Determination of $\Delta C_p$ allowed extrapolation of thermodynamic parameters at any given temperature, $T$, using the eqs 6, 7 and 8. A complete thermodynamic profile for heteroduplex formation at 37 °C has been depicted in Table 3. As evident from the tabulated values heteroduplex formation is associated with a favorable enthalpy change (negative $\Delta H$) and unfavorable entropy change (a negative $\Delta S$). The slope of the plot between $\Delta H$ and $\Delta S$, depicted in Supporting Information, Figure SI4, gave the compensation temperature, $T_c$, of 400 K (127 °C), which lay far beyond our experimental temperature. This significant difference between $T_c$ and our experimental temperature indicated a statistically relevant "compensation" between the

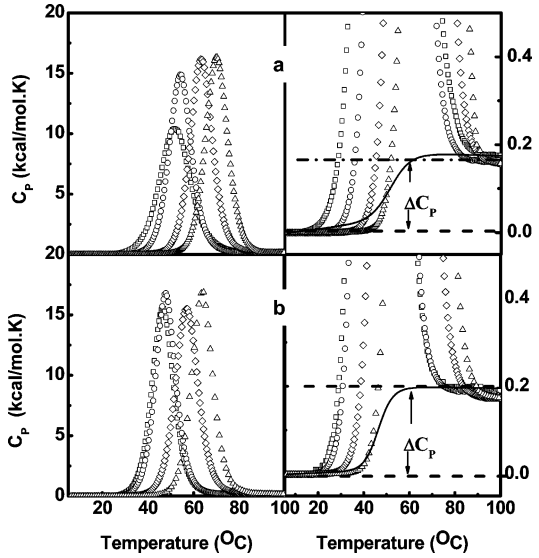


FIGURE 2: Typical DSC curves of the heteroduplex melting in 10 mM sodium cacodylate buffer (pH 7.0), for (a) T-LNA0 (□), T-LNA1 (○), T-LNA2 (◇), T-LNA3 (△) and (b) A-LNA0 (□), A-LNA1 (○), A-LNA2 (◇), A-LNA3 (△). The right panel describes estimation of $\Delta C_p$ by extrapolation of pre- and postdenaturation baselines to midpoint of transition. Each experiment consists of heating of a sample cell containing 0.52 mL of 30 $\mu$M heteroduplex solution and a reference cell filled with the same volume of buffer, in the temperature range 10 to 90 °C at a rate of 1 °C/min.

enthalpy and the entropy parameter (*52*, *53*). The influence of LNA-substitution on thermodynamic parameters, with respect to the unmodified duplex, is also depicted ($\Delta\Delta H$, $\Delta\Delta S$ and $\Delta\Delta G$). It appears that introduction of an extra LNA-modification in DNA strand of the heteroduplex leads to an increase in the favorable enthalpy term. Similar to our UV-melting data, in DSC also, we observed a higher $T_m$ increment by T-LNA substitution relative to an A-LNA. A similar trend could also be observed in the overall free energy parameter ($\Delta G°$), suggesting a higher stabilization by thymine substituted-LNA than an adenine substitution.

*ITC Studies for Duplex Formation.* A complete thermodynamic profile for the association of LNA-modified DNA strand with RNA, as summarized in Table 4, was determined by ITC at 10 °C. In the case of ITC, ideal experimental conditions for determining $\Delta H$ accurately are high concentrations so as to have saturation binding, while ideal experimental conditions for determining $\Delta G$ accurately are low concentrations to have a smooth equilibrium binding curve. As presented in Figure 3, in all cases the stoichiometry $n$ was approximately equivalent to unity. The respective binding affinity between the two complementary strands, depicted by $K_a$ and the exothermic enthalpy change ($\Delta H_{ITC}$) for formation of duplex was observed to increase with increase in the number of LNA substitutions, indicating an increase in the stability of the LNA modified duplex. This trend in enthalpy change correlated well with our DSC data. The binding affinity and the corresponding enthalpy change for each duplex was then used to furnish other thermodynamic parameters (Table 4) at 10 °C, using eq 9. It can be noted that the binding affinity can be determined accurately only when titrant is added to a fixed concentration [$C_0$] of complementary strand, such that it lies in the range of $1/K_A$; otherwise the obtained $K_A$ would be underestimated. However, the ITC experiment here was performed at [$C_0$] 30 (T-LNA) and 15 $\mu$M, (A-LNA) which is much higher than $1/K_A$ values obtained from the analysis. An ITC experiment at low DNA concentration ($\sim 1/K_A$) would give a heat of reaction below the sensitivity of the instrument.

*Counterion Uptake upon Duplex Formation*. To estimate the effect of LNA modification on the counterion uptake associated with the process of duplex formation, UV melting curves of duplexes (2 $\mu$M) at several salt concentrations (10−110 mM $Na^+$) were studied. A representative curve for A-LNA3 and T-LNA3 has been provided in Supporting Information, Figure SI5. The dependence of $T_m$ on salt concentration for each heteroduplex is also shown (Figure 4). The slopes of these curves are listed in Table 5. Sodium ions contribute to the stability of helical structures by reducing the repulsive forces between phosphate groups along the chain (*54*), and therefore, increasing the sodium ion concentration from 10 mM to 110 mM results in the shift of melting curves to higher $T_m$ values. Furthermore, the charge density of double-helix is known to be higher than single stranded oligonucleotides; as a result the transition from a single stranded to a helical state (duplex formation) is always accompanied by a net uptake of $Na^+$ ions (*55*). In the case of LNA-modified heteroduplexes, we observed that introduction of the modification into one of the strands of the duplex leads to a higher uptake of counterions (sodium ions) upon duplex formation. The counterion uptake for each heteroduplex (Table 5) over this range of salt concentration was calculated using eq 4 and is listed in Table 5.

*Uptake of Water Molecules upon Duplex Formation*. To detect the differences in the hydration of the heteroduplexes induced by the incorporation of LNA nucleotide modifications, we employed an osmotic stressing method (*56*, *57*). The technique involves use of low molecular weight cosolute (osmolyte) that itself does not interact with the biopolymer but produces changes in the water activity ($a_W$). Monitoring the change in $T_m$ of the double-helix as a function of change in water activity gives the number of water molecules that are uniquely bound to helix and are released upon melting or unfolding of the duplex (*45*). We used a different concentration range (0−25%) of ethylene glycol (osmolyte) at 100 mM NaCl to monitor the $T_m$ dependence of heteroduplexes on water activity. A representative curve for A-LNA3 and T− LNA3 is shown in Supporting Information, Figure SI6. In each case, the increase in the osmolyte concentration shifts the $T_m$ of melting curves to lower temperatures. The $1/T_m$ dependence on ln $a_W$ is shown in Figure 5 for each heteroduplex. The extent of water uptake upon formation of the duplex was calculated using eq 5. The slope of these plots, along with the corresponding change in the number of water molecules taken up by the duplexes, is given in Table 5. It was observed that increasing the number of LNA nucleotides led to a lower uptake of water molecules by the modified duplexes as compared to the unmodified duplex, suggesting that the modified duplexes are less hydrated than their corresponding unmodified counterparts.

## DISCUSSION

We have used UV, DSC and ITC measurements to extensively study the hybridization thermodynamics of LNA-

Table 3: Thermodynamic Parameters Obtained by DSC for the Formation of Duplexes[a]

| duplex | $T_m$ °C | $\Delta H_m$ kcal/mol | $\Delta C_p$ cal/mol·K | $\Delta H_{(37°C)}$ kcal/mol | $\Delta S_{(37°C)}$ eu | $\Delta G_{(37°C)}$ kcal/mol | $\Delta\Delta H_{(37°C)}$ kcal/mol | $\Delta\Delta S_{(37°C)}$ eu | $\Delta\Delta G_{(37°C)}$ kcal/mol |
|---|---|---|---|---|---|---|---|---|---|
| T-LNA0 | 51.7 | −55.0 | −173 | −57.5 | −177 | −2.5 | | | |
| T-LNA1 | 54.3 | −64.0 | −165 | −66.8 | −204 | −3.4 | −9.3 | −27 | −6.2 |
| T-LNA2 | 63.4 | −69.4 | −168 | −73.8 | −220 | −5.6 | −16.2 | −42 | −8.3 |
| T-LNA3 | 70.1 | −71.7 | −155 | −76.8 | −224 | −7.1 | −19.2 | −47 | −10.0 |
| A-LNA0 | 46.5 | −63.0 | −193 | −64.8 | −203 | −1.9 | | | |
| A-LNA1 | 47.5 | −66.0 | −175 | −67.8 | −211 | −2.2 | −3.0 | −8 | −4.2 |
| A-LNA2 | 56.8 | −67.8 | −195 | −71.6 | −217 | −4.1 | −6.8 | −14 | −6.2 |
| A-LNA3 | 63.8 | −71.4 | −180 | −76.2 | −226 | −5.8 | −11.4 | −23 | −8.0 |

[a] All the parameters were obtained from DSC experiments conducted in 10 mM sodium cacodylate buffer (pH 7.0). Heteroduplex concentrations were 30 $\mu$M. $T_m$ values are within ±0.5 °C, $\Delta H_m$ values are within 3%, and $\Delta G$ and $\Delta S$ values are within 5% error obtained from three experimental replicas.

Table 4: Thermodynamic Parameters Obtained by ITC for the Formation of Duplexes at 10 °C[a]

| duplex | $\Delta H_{ITC}$ kcal/mol | $\Delta S$ eu | $\Delta G^o$ (10 °C) kcal/mol | $K_a$ |
|---|---|---|---|---|
| T-LNA0 | −49.7 | −144 | −8.9 | $8.58 \times 10^6$ |
| T-LNA1 | −60.0 | −180 | −9.0 | $9.73 \times 10^6$ |
| T-LNA2 | −66.3 | −201 | −9.3 | $1.54 \times 10^7$ |
| T-LNA3 | −72.4 | −221 | −9.8 | $3.80 \times 10^7$ |
| A-LNA0 | −60.0 | −180 | −8.8 | $7.24 \times 10^6$ |
| A-LNA1 | −62.1 | −187 | −9.0 | $9.52 \times 10^6$ |
| A-LNA2 | −65.0 | −195 | −9.9 | $3.67 \times 10^7$ |
| A-LNA3 | −67.0 | −201 | −10.1 | $6.59 \times 10^7$ |

[a] All the parameters were obtained from ITC experiments, conducted in 10 mM sodium cacodylate buffer (pH 7.0). DNA strand concentration in cell was 30 $\mu$M for T-LNA and 15 $\mu$M for A-LNA set, while RNA concentration in syringe was 300 $\mu$M and 150 $\mu$M for T-LNA and A-LNA set, respectively. $\Delta H$, $\Delta S$ and $\Delta G$ values are within 5% error, while $K_a$ values are within 10% error, obtained from three experimental replicas.

modified heteroduplexes. In our UV-studies we observed that few of our heteroduplexes had melting temperature close to 25−30 °C; thus we chose to perform our ITC experiments at 10 °C where all the duplexes existed in the helical state. The DSC analysis provided enthalpy change associated with duplex unfolding near melting temperature. However, biological application of these modified oligonucleotides would involve extrapolation of these thermodynamic parameters to the relevant experimental temperature. This is particularly important in the case of LNA-modified oligonucleotides that have wide applications, ranging from antisense-therapeutics that commonly work at 37 °C to diagonostic probes in PCR reactions with working range of about 55−90 °C. A prior knowledge of heat capacity change ($\Delta C_p$) associated with helix-to-coil transition is thus required to account for the temperature dependence of $\Delta H$ and $\Delta S$. This consideration becomes important in view of a large body of experimental and theoretical evidence suggesting that helix-to-coil transitions of nucleic acids are accompanied by changes in heat capacity and that failure to account for this change leads to errors in estimation of true $\Delta H$ and $\Delta S$ values, at temperatures distant from the melting temperature (*46*, *47*, *58*−*60*). Analysis of our DSC melting curves allowed estimation of $\Delta C_p$ accompanying the helix to coil transitions of these heteroduplexes (*50*, *51*). The average value of $\Delta C_p$ was found to be 175.5 cal·mol$^{-1}$ K$^{-1}$, which is equivalent to 22 cal·(mol of base pairs)$^{-1}$ K$^{-1}$. Our $\Delta C_p$ values are, thus, in qualitative agreement with the literature values of 64 cal·(mol of base pairs)$^{-1}$ K$^{-1}$ for long polymeric nucleic acids and an average value of 36 cal·(mol of base pairs)$^{-1}$ K$^{-1}$ (*46*, *47*) observed for small duplexes. The lower $\Delta C_p$ values in our case might be because of smaller size of our duplexes. This $\Delta C_p$ value could be used to accurately determine $\Delta H$ and $\Delta S$ values at any given experimental temperature. We have used this value to deduce complete thermodynamic parameters at 37 °C (Table 3). A close analysis of the obtained $\Delta H$ and $\Delta S$ values indicated that favorable folding of duplex in our case results from compensation of the favorable enthalpy term and the unfavorable entropy term. While the unfavorable entropy contribution stems mainly from the conformational rearrangement of the bimolecular association of two strands, and the uptake of counterions and water molecules, the favorable enthalpy term corresponds to exothermic contributions of base pairing and base pair stacking interactions. A modification such as an LNA substitution in an oligonucleotide may contribute to either enthalpy or entropy change, or both, in free energy ($\Delta G$) relative to the unmodified duplex. Complete thermodynamic profile obtained from ITC and DSC measurements suggest that the increased stability of RNA·LNA/DNA heteroduplexes compared to RNA·DNA heteroduplexes originates from the increase in the favorable enthalpy term that overrides the effect of the unfavorable entropy change. The overall effect indicates that modified duplexes have a larger exothermic contribution than the unmodified duplexes, indicating that base stacking interactions in the modified duplexes are more pronounced. Our ITC data also demonstrated an increase in binding affinity ($K_a$) of two strands, associated with increase in the LNA-content of the heteroduplex. Compared to an adenine-substituted-modification (A-LNA), a more significant influence of LNA-substitution, in terms of thermostability and binding affinity was observed when the substitution was incorporated at the 'thymine' residue (T-LNA) of the DNA strand. In other words, a thymine substitution is more sensitive to the effect of LNA as compared to an adenine substitution.

The presence of counterions associated with nucleic acids is a significant factor influencing their stability. During the process of duplex formation there is a net uptake of counterions, which in turn affects the overall stability of the helix. Investigating the change in the number of counterions ($\Delta\Delta n_{Na^+}$) associated with an LNA-modified heteroduplex, with respect to the unmodified heteroduplex, will aid in elucidating the origin of stability for LNA-based oligonucleotides. Our study demonstrates an increased uptake of counterions consistent with an increase in the LNA-content of the DNA strand. This finding can be ascribed to the LNA-

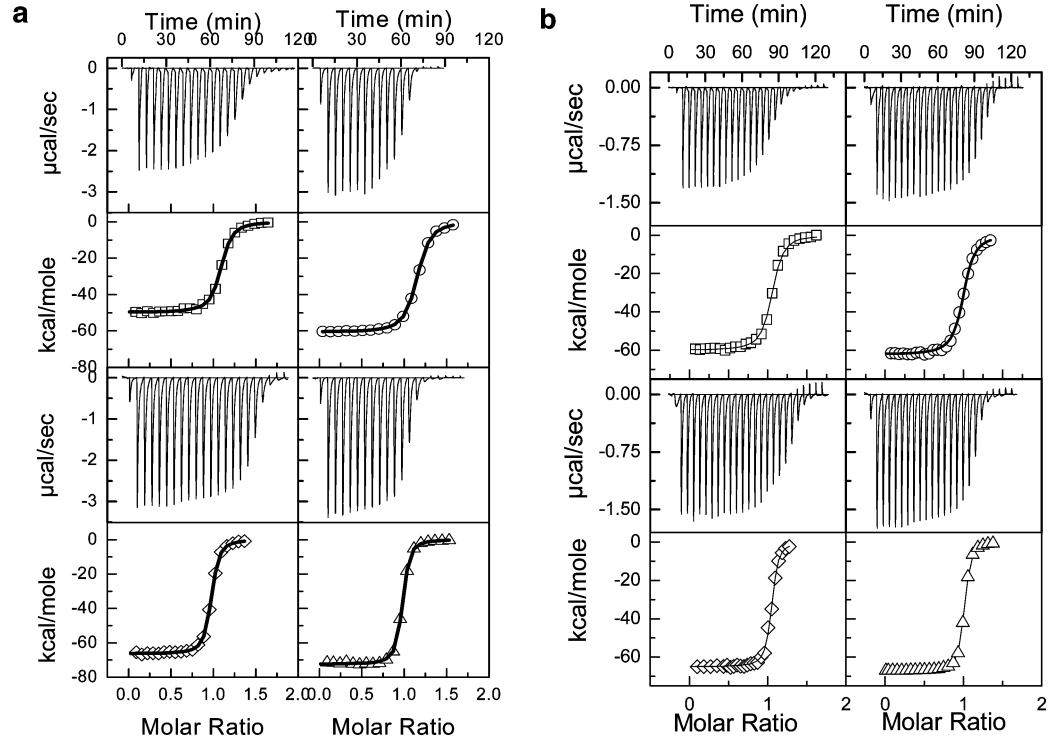


FIGURE 3: ITC curves of the heteroduplex formation in 10 mM sodium cacodylate buffer (pH 7.0), for (a) T-LNA0 (□), T-LNA1 (○), T-LNA2 (◇), T-LNA3 (△) and (b) A-LNA0 (□), A-LNA1 (○), A-LNA2 (◇), A-LNA3 (△). For each titration, the DNA strand with concentration 30 $\mu$M for T-LNA and 15 $\mu$M for A-LNA was loaded into a 1.4 mL sample cell, and the complementary RNA strand at concentration 300 $\mu$M for T-LNA and 150 $\mu$M for A-LNA was loaded into the 250 $\mu$L injection syringe and 10 $\mu$L was injected in each time at the stirring rate of 400 rpm.

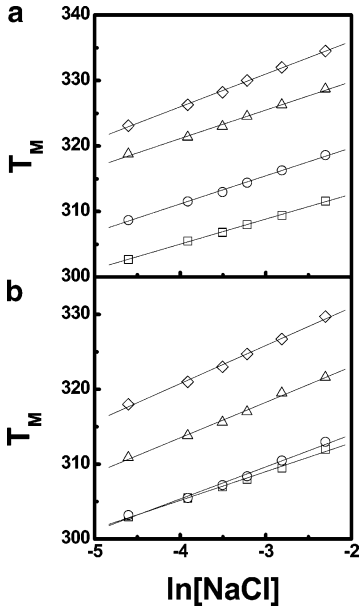


FIGURE 4: $T_m$ dependence on salt concentration is shown for (a) T-LNA0 (□), T-LNA1 (○), T-LNA2 (△), T-LNA3 (◇) and for (b) A-LNA0 (□), A-LNA1 (○), A-LNA2 (△), A-LNA3 (◇).

induced conformation change of the helix to an A-type geometry. Literature findings on structural characterization of LNA/DNA·RNA hybrids have revealed an increasing A-like conformation in the hybrid as the LNA content of the modified strand is increased (*61*, *62*). This is attributed to the LNA-induced structural perturbation of the DNA nucleotides in the LNA strand to attain an N-type sugar pucker, which contrasts with the equilibrium between the N- and S-type sugar conformations in the native DNA·RNA duplex. The increase in the population of N-type sugar puckers in the hybrid forces an A-like geometry that progressively increases with an increase in LNA content (*61*, *62*). Furthermore, both the linear and three-dimensional charge density of an A-form helix are known to be higher than that of the B-form (*44*). Compared to the unmodified heteroduplexes, the higher charge density of LNA-modified heteroduplexes (A-form helix) leads to a higher uptake of counterions upon duplex formation. Further, this increase in the uptake of counterions by the duplex possibly accounts for the unfavorable entropy change associated with the introduction of LNA modification.

Water is an integral part of nucleic acid structure (*63*−*67*), and therefore, understanding the effects of hydration on the chemical and physical properties of DNA depends on evaluation of the quantity of water bound and how the water content changes when DNA undergoes physical or chemical change (*66*, *68*). The knowledge of the hydration changes due to the LNA modification will additionally allow us to identify the origin of enhanced thermal stability of the LNA-modified duplexes. Extensive hydration of the negative phosphate oxygens is seen for both A- and B-DNA. However, the two forms of duplex differ considerably with respect to the extent of hydration and arrangement of water molecules in the major and minor grooves. The hydration of phosphates in B-DNA is isolated, whereas it overlaps in A-DNA (*68*−*71*). The more economical hydration of phosphates, along with loss of spine of hydration in A-form is responsible for the transition of B-DNA to A-DNA when water activity is lowered (*72*). Because of the 2′-OH group, the hydration of A-RNA is changed considerably and

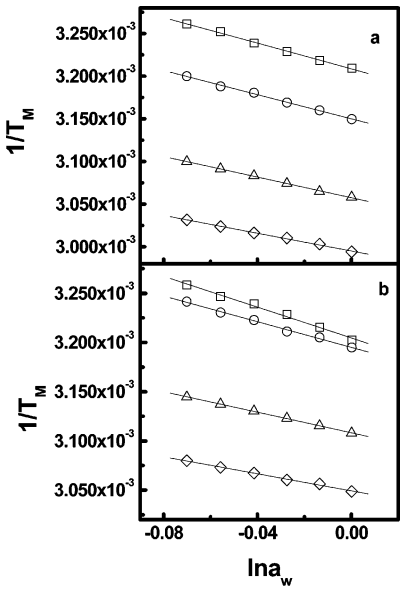


FIGURE 5: Dependence of $1/T_m$ on ln $a_W$ for (a) T-LNA0 (□), T-LNA1 (○), T-LNA2 (△), T-LNA3 (◇) and for (b) A-LNA0 (□), A-LNA1 (○), A-LNA2 (△), A-LNA3 (◇).

Table 5: Thermodynamic Uptake of Counterions and Water Molecules upon Formation of Duplex[a]

| duplex | $\delta T_m/\delta Na^+$ | $\Delta n_{Na^+}$ (per duplex) | $\delta(1/T_m)/\delta(\ln a_W)$ | $\Delta n_W$ (per duplex) | $\Delta\Delta n_{Na+}$ | $\Delta\Delta n_W$ |
|---|---|---|---|---|---|---|
| T-LNA0 | 3.7 | −2.6 | $-7.65 \times 10^{-4}$ | 23.6 | | |
| T-LNA1 | 4.0 | −2.8 | $-6.86 \times 10^{-4}$ | 23.2 | −0.2 | −0.4 |
| T-LNA2 | 4.2 | −3.0 | $-5.89 \times 10^{-4}$ | 21.4 | −0.4 | −2.2 |
| T-LNA3 | 4.8 | −3.5 | $-5.16 \times 10^{-4}$ | 19.2 | −0.9 | −4.4 |
| A-LNA0 | 3.7 | −2.7 | $-7.81 \times 10^{-4}$ | 25.3 | | |
| A-LNA1 | 4.3 | −3.1 | $-6.60 \times 10^{-4}$ | 21.6 | −0.4 | −3.7 |
| A-LNA2 | 4.5 | −3.3 | $-6.08 \times 10^{-4}$ | 18.0 | −0.6 | −7.3 |
| A-LNA3 | 5.10 | −3.7 | $4.82 \times 10^{-4}$ | 15 | −1.0 | −10.3 |

[a] Experiments were conducted with 2 $\mu$M heteroduplex concentration in 10 mM sodium cacodylate buffer, at pH 7.0, and adjusted to different concentrations of sodium chloride or ethylene glycol. Experiments with ethylene glycol were conducted in 10 mM sodium cacodylate buffer containing 100 mM $Na^+$. $\delta T_m/\delta Na^+$ and $\delta(1/T_m)/\delta(\ln a_W)$ values are within 5%, and $\Delta n_{Na^+}$ and $\Delta n_W$ values are within 10% error.

displays conserved regular arrangement of water in both the grooves (*73*). The 2′-OH group is suggested to stabilize the RNA duplex by reinforcing the A-type geometry and by linking backbone and base hydration across the strands (*72*). Thus, the greater thermal stability of RNA or RNA/DNA hetroduplex (due to greater stabilization enthalpy) compared to DNA duplexes emanates from the 2′-OH of the RNA acting both as a scaffold for the water network in the minor groove and as a site of extensive individual hydration. This fact accounts for the higher $T_m$ and enthalpy change observed for LNA/DNA·RNA heteroduplexes, compared to LNA/DNA·DNA duplexes used in our previous study (*40*). A corollary to the above is that the melting of an A-type DNA·RNA heteroduplex will release a higher number of water molecules than the melting of DNA·DNA duplex. Our data supports this fact as we observed a higher uptake of water molecules associated with LNA/DNA·RNA heteroduplex formation compared to LNA/DNA·DNA duplex, used in previous study. Furthermore, within the LNA-modified heteroduplexes, the uptake of water molecules decreased as the LNA content of the hetroduplex was increased (Table 5). This can again be attributed to the LNA-induced structural perturbation of the heteroduplex that drives the hybrid to an A-type geometry, which is much more dehydrated than the respective unmodified hybrid. The number of water molecules taken up, thus, decreases with an increase in LNA content.

## CONCLUSION

Considering the increasing success of LNA-technology in hybridization-based assays involving RNA as the target, we have attempted to study the influence of LNA substitution on the hybridization thermodynamics, counterions, and hydration DNA·RNA heteroduplex. Thermal denaturation experiments with differentially modified heteroduplexes suggested a higher thermal stability for the modified duplexes. We conclude that this increased stability of LNA-modified duplexes mainly emanates from the increase in hybridization efficiency of the complementary strands, as indicated by our ITC data. Analysis of the DSC data allowed estimation of $\Delta C_p$ change accompanying each duplex formation, which could further be extrapolated to obtain thermodynamic parameters at any given experimental temperature condition. Thermodynamically, the presence of extra LNA-substitution produces a larger increase in the favorable enthalpy term that overrides the effect of unfavorable entropy, thereby making the overall process of LNA-heteroduplex formation energetically more favorable than unmodified heteroduplex. Among the adenine (A-LNA) and thymine (T-LNA) substitutions, a slightly higher increment in thermal stability and binding affinity was observed for the thymine modified heteroduplexes. Furthermore, the optical melting data showed that the formation of modified heteroduplexes is associated with higher counterion uptake and a relatively lower uptake of water molecules as compared to the unmodified heteroduplex. This observation can be ascribed to the LNA induced structural perturbation of the helical geometry that drives the helix to assume A-type conformation that possesses a higher charge density but is less hydrated than the B-type conformation of the unmodified duplexes. Our study is a preliminary attempt for the realization of creating a probe dataset that would allow highly sensitive and robust detection or targeting of target RNA. Efficient designing of these probe sets, however, calls for extensive evaluation and characterization of biophysical properties of LNA-based oligonucleotides in different sequence contexts. In the near future, we hope to investigate the effect of LNA modification on hybridization thermodynamics as a function of LNA content, sequence composition, the neighboring bases flanking the modification, the target length and structure. Tracking the effects of LNA modifications in the aforementioned contexts will allow us to formulate guidelines for the optimum design of LNA-based oligonucleotides such that maximum functional efficiency could be drawn out of minimum modification.

## ACKNOWLEDGMENT

H.K. thanks ICMR for providing the fellowship grant. J.W. thanks The Danish National Research Foundation for funding The Nucleic Acid Center. The authors are thankful to the esteemed referee for providing valuable suggestions to improve the manuscript.

## SUPPORTING INFORMATION AVAILABLE

Figures SI1−7 depicting hysteresis curves, melting curves, and an enthalpy/entropy compensation plot. This material is available free of charge via the Internet at http://pubs.acs.org.

## REFERENCES


1. Kurreck, J. (2003) Antisense technologies. Improvement through novel chemical modifications, *Eur. J. Biochem. 270*, 1628−1644.
2. Petersen, M., and Wengel, J. (2003) LNA: a versatile tool for therapeutics and genomics, *Trends Biotechnol. 21*, 74−81.
3. Kurreck, J., Wyszko, E., Gillen, C., and Erdmann, V. A. (2002) Design of antisense oligonucleotides stabilized by locked nucleic acids, *Nucleic Acids Res. 30*, 1911−1918.
4. Wengel, J., Petersen, M., Nielsen, K. E., Jensen, G. A., Hakansson, A. E., Kumar, R., Sorensen, M. D., Rajwanshi, V. K., Bryld, T., and Jacobsen, J. P. (2001) LNA (locked nucleic acid) and the diastereoisomeric alpha-L-LNA: conformational tuning and high-affinity recognition of DNA/RNA targets, *Nucleosides Nucleotides Nucleic Acids 20*, 389−396.
5. Koshkin, A. A., Nielsen, P., Meldgaard, M., Rajwanshi, V. K., Singh, S. K., and Wengel, J. (1998) LNA (Locked Nucleic Acid): An RNA mimic forming exceedingly stable LNA:LNA duplexes, *J. Am. Chem. Soc. 120*, 13252−13253.
6. Kaur, H., Wengel, J., and Maiti, S. (2007) LNA-modified oligonucleotides effectively drive intramolecular-stable hairpin to intermolecular-duplex state, *Biochem. Biophys. Res. Commun. 352*, 118−122.
7. Schmidt, K. S., Borkowski, S., Kurreck, J., Stephens, A. W., Bald, R., Hecht, M., Friebe, M., Dinkelborg, L., and Erdmann, V. A. (2004) Application of locked nucleic acids to improve aptamer in vivo stability and targeting function, *Nucleic Acids Res. 32*, 5757−5765.
8. Hansen, J. B., Westergaard, M., Thrue, C. A., Giwercman, B., and Oerum, H. (2003) Antisense knockdown of PKC-alpha using LNA-oligos, *Nucleosides Nucleotides Nucleic Acids 22*, 1607−1609.
9. Fluiter, K., ten Asbroek, A. L., de Wissel, M. B., Jakobs, M. E., Wissenbach, M., Olsson, H., Olsen, O., Oerum, H., and Baas, F. (2003) In vivo tumor growth inhibition and biodistribution studies of locked nucleic acid (LNA) antisense oligonucleotides, *Nucleic Acids Res. 31*, 953−962.
10. Obika, S., Hemamayi, R., Masuda, T., Sugimoto, T., Nakagawa, S., Mayumi, T., and Imanishi, T. (2001) Inhibition of ICAM-1 gene expression by antisense 2′,4′-BNA oligonucleotides, *Nucleic Acids Res. Suppl.* 145−146.
11. Childs, J. L., Disney, M. D., and Turner, D. H. (2002) Oligonucleotide directed misfolding of RNA inhibits Candida albicans group I intron splicing, *Proc. Natl. Acad. Sci. U.S.A. 99*, 11091−11096.
12. Elayadi, A. N., Braasch, D. A., and Corey, D. R. (2002) Implications of high-affinity hybridization by locked nucleic acid oligomers for inhibition of human telomerase, *Biochemistry 41*, 9973−9981.
13. Arzumanov, A., Walsh, A. P., Liu, X., Rajwanshi, V. K., Wengel, J., and Gait, M. J. (2001) Oligonucleotide analogue interference with the HIV-1 Tat protein-TAR RNA interaction, *Nucleosides Nucleotides Nucleic Acids 20*, 471−480.
14. Frieden, M., Hansen, H. F., and Koch, T. (2003) Nuclease stability of LNA oligonucleotides and LNA-DNA chimeras, *Nucleosides Nucleotides Nucleic Acids 22*, 1041−1043.
15. Simoes-Wust, A. P., Hopkins-Donaldson, S., Sigrist, B., Belyanskaya, L., Stahel, R. A., and Zangemeister-Wittke, U. (2004) A functionally improved locked nucleic acid antisense oligonucleotide inhibits Bcl-2 and Bcl-xL expression and facilitates tumor cell apoptosis, *Oligonucleotides 14*, 199−209.
16. Zangemeister-Wittke, U. (2003) Antisense to apoptosis inhibitors facilitates chemotherapy and TRAIL-induced death signaling, *Ann. N.Y. Acad. Sci. 1002*, 90−94.
17. Nulf, C. J., and Corey, D. (2004) Intracellular inhibition of hepatitis C virus (HCV) internal ribosomal entry site (IRES)-dependent translation by peptide nucleic acids (PNAs) and locked nucleic acids (LNAs), *Nucleic Acids Res. 32*, 3792−3798.
18. Arzumanov, A., Walsh, A. P., Rajwanshi, V. K., Kumar, R., Wengel, J., and Gait, M. J. (2001) Inhibition of HIV-1 Tat-dependent trans activation by steric block chimeric 2′-O-methyl/LNA oligoribonucleotides. *Biochemistry 40*, 14645−14655.
19. Arzumanov, A., Stetsenko, D. A., Malakhov, A. D., Reichelt, S., Sorensen, M. D., Babu, B. R., Wengel, J., and Gait, M. J. (2003) A structure-activity study of the inhibition of HIV-1 Tat-dependent trans-activation by mixmer 2′-O-methyl oligoribonucleotides containing locked nucleic acid (LNA), alpha-L-LNA, or 2′-thio-LNA residues, *Oligonucleotide 13*, 435−453.
20. Darfeuille, F., Reigadas, S., Hansen, J. B., Orum, H., Di, P. C., and Toulme, J. J. (2006) Aptamers targeted to an RNA hairpin show improved specificity compared to that of complementary oligonucleotides, *Biochemistry 45*, 12076−12082.
21. Elmen, J., Zhang, H. Y., Zuber, B., Ljungberg, K., Wahren, B., Wahlestedt, C., and Liang, Z. (2004) Locked nucleic acid containing antisense oligonucleotides enhance inhibition of HIV-1 genome dimerization and inhibit virus replication, *FEBS Lett. 578*, 285−290.
22. Mong, J. A., Devidze, N., Goodwillie, A., and Pfaff, D. W. (2003) Reduction of lipocalin-type prostaglandin D synthase in the preoptic area of female mice mimics estradiol effects on arousal and sex behavior, *Proc. Natl. Acad. Sci. U.S.A. 100*, 15206−15211.
23. Charlier, T. D., Ball, G. F., and Balthazart, J. (2006) Plasticity in the expression of the steroid receptor coactivator 1 in the Japanese quail brain: effect of sex, testosterone, stress and time of the day, *Neuroscience 140*, 1381−1394.
24. Thomsen, R., Nielsen, P. S., and Jensen, T. H. (2005) Dramatically improved RNA in situ hybridization signals using LNA-modified probes, *RNA 11*, 1745−1748.
25. Orom, U. A., Kauppinen, S., and Lund, A. H. (2006) LNA-modified oligonucleotides mediate specific inhibition of microRNA function, *Gene 372*, 137−141.
26. Wienholds, E., and Plasterk, R. H. (2005) MicroRNA function in animal development, *FEBS Lett. 579*, 5911−5922.
27. Kloosterman, W. P., Wienholds, E., de, B. E., Kauppinen, S., and Plasterk, R. H. (2006) In situ detection of miRNAs in animal embryos using LNA-modified oligonucleotide probes, *Nat. Methods 3*, 27−29.
28. Neely, L. A., Patel, S., Garver, J., Gallo, M., Hackett, M., McLaughlin, S., Nadel, M., Harris, J., Gullans, S., and Rooke, J. (2006) A single-molecule method for the quantitation of microRNA gene expression, *Nat. Methods. 3*, 41−46.
29. Castoldi, M., Schmidt, S., Benes, V., Noerholm, M., Kulozik, A. E., Hentze, M. W., and Muckenthaler, M. U. (2006) A sensitive array for microRNA expression profiling (miChip) based on locked nucleic acids (LNA), *RNA 12*, 913−920.
30. Nelson, P. T., Baldwin, D. A., Kloosterman, W. P., Kauppinen, S., Plasterk, R. H., and Mourelatos, Z. (2006) RAKE and LNA-ISH reveal microRNA expression and localization in archival human brain, *RNA 12*, 187−191.
31. Naguibneva, I., meyar-Zazoua, M., Nonne, N., Polesskaya, A., it-Si-Ali, S., Groisman, R., Souidi, M., Pritchard, L. L., and Harel-Bellan, A. (2006) An LNA-based loss-of-function assay for microRNAs, *Biomed. Pharmacother. 60*, 633−638.
32. Wengel, J. (1999) Synthesis of 3′-C- and 4-C-branched oligodeoxynucleotides and the development of locked nucleic acids (LNA), *Acc. Chem. Res. 32*, 301.
33. Braasch, D. A., and Corey, D. R. (2001) Locked nucleic acid (LNA): fine-tuning the recognition of DNA and RNA, *Chem. Biol. 8*, 1−7.
34. Kvaerno, L., Kumar, R., Dahl, B. M., Olsen, C. E., and Wengel, J. (2000) Synthesis of abasic locked nucleic acid and two seco-LNA derivatives and evaluation of their hybridization properties compared with their more flexible DNA counterparts, *J. Org. Chem. 65*, 5167−5176.
35. Koshkin, A. A., Singh, S. K., Nielsen, P., Rajwanshi, V. K., Kumar, R., Meldgaard, M., Olsen, C. E. and Wengel, J. (1998) LNA (Locked Nucleic Acids) synthesis of the Adenine, Cytosine, Guanine, 5-Methylcytosine, Thymine and Uracil bicyclonucleoside monomers, oligomerisation, and unprecedented nucleic acid recognition, *Tetrahedron* 54, 3607−3630.
36. Obika, S., Nanbu, D., Hari, Y., Morio, J. A. K., Doi, T., and Imanishi, T. (1998) Stability and structural features of the duplexes containing nucleoside analogues with a fixed N-type conformation, 2′-O,4′-C-methyleneribonucleosides, *Tetrahedron Lett. 39*, 5401−5404.
37. Christensen, U., Jacobsen, N., Rajwanshi, V. K., Wengel, J., and Koch, T. (2001) Stopped-flow kinetics of locked nucleic acid (LNA)-oligonucleotide duplex formation: studies of LNA-DNA and DNA-DNA interactions, *Biochem. J. 354*, 481−484.

38. McTigue, P. M., Peterson, R. J., and Kahn, J. D. (2004) Sequence-dependent thermodynamic parameters for locked nucleic acid (LNA)-DNA duplex formation, *Biochemistry 43*, 5388−5405.
39. Kierzek, E., Ciesielska, A., Pasternak, K., Mathews, D. H., Turner, D. H., and Kierzek, R. (2005) The influence of locked nucleic acid residues on the thermodynamic properties of 2′-O-methyl RNA/RNA heteroduplexes, *Nucleic Acids Res. 33*, 5082−5093.
40. Kaur, H., Arora, A., Wengel, J., and Maiti, S. (2006) Thermodynamic, counterion, and hydration effects for the incorporation of locked nucleic acid nucleotides into DNA duplexes, *Biochemistry 45*, 7347−7355.
41. Marky, L. A., Blumenfeld, K. S., Kozlowski, S., and Breslauer, K. J. (1983) Salt-dependent conformational transitions in the self-complementary deoxydodecanucleotide d(CGCAATTCGCG): evidence for hairpin formation, *Biopolymers 22*, 1247−1257.
42. McDowell, J. A., and Turner, D. H. (1996) Investigation of the structural basis for thermodynamic stabilities of tandem GU mismatches: Solution structure of $(rGAGGUCUC)_2$ by two-dimensional NMR and simulated annealing, *Biochemistry* 35, 14077−14089.
43. Mergny, J. L., and Lacroix, L. (2003) Analysis of thermal melting curves, *Oligonucleotides 13*, 515−537.
44. Rentzeperis, D., Kharakoz, D. P., and Marky, L. A. (1991) Coupling of sequential transitions in a DNA double hairpin: energetics, ion binding, and hydration, *Biochemistry 30*, 6276−6283.
45. Spink, C. H., and Chaires, J. B. (1999) Effects of hydration, ion release, and excluded volume on the melting of triplex and duplex DNA, *Biochemistry 38*, 496−508.
46. Chalikian, T. V., Volker, J., Plum, G. E., and Breslauer, K. J. (1999) A more unified picture for the thermodynamics of nucleic acid duplex melting: a characterization by calorimetric and volumetric techniques, *Proc. Natl. Acad. Sci. U.S.A. 96*, 7853−7858.
47. Tikhomirova, A., Beletskaya, I. V., and Chalikian, T. V. (2006) Stability of DNA duplexes containing GG, CC, AA, and TT mismatches, *Biochemistry 45*, 10563−10571.
48. Soto, A. M., Kankia, B. I., Dande, P., Gold, B., and Marky, L. A. (2002) Thermodynamic and hydration effects for the incorporation of a cationic 3-aminopropyl chain into DNA, *Nucleic Acids Res. 30*, 3171−3180.
49. Soto, A. M., Kankia, B. I., Dande, P., Gold, B., and Marky, L. A. (2001) Incorporation of a cationic aminopropyl chain in DNA hairpins: thermodynamics and hydration, *Nucleic Acids Res. 29*, 3638−3645.
50. Rouzina, I., and Bloomfield, V. A. (1999) Heat capacity effects on the melting of DNA. 1. General aspects, *Biophys. J. 77*, 3242−3251.
51. Tikhomirova, A., Taulier, N., and Chalikian, T. V. (2004) Energetics of nucleic acid stability: the effect of Delta $C_P$, *J. Am. Chem. Soc. 126*, 16387−16394.
52. Lei, L., and Guo, Q.-X. (2001) Isokinetic Relationship, and Enthalpy-Entropy Compensation, *Chem. Rev. 101*, 673−695.
53. Krug, R. R., Hunter, W. G., and Greiger, R. A. (1976) Statistical interpretation of enthalpy-entropy compensation, *Nature 261*, 566−567.
54. Manning, G. S. (2002) Electrostatic free energy of the DNA double helix in counterion condensation theory, *Biophys. Chem. 101−102*, 461−473.
55. Jayaram, B., Sprous, D., Young, M. A., and Beveridge, D. L. (1998) Free energy analysis of the conformational preferences of A and B forms of DNA in solution, *J. Am. Chem. Soc. 120*, 10629−10633.
56. Zieba, K., Chu, T. M., Kupke, D. W., and Marky, L. A. (1991) Differential hydration of dA.dT base pairing and dA and dT bulges in deoxyoligonucleotides, *Biochemistry 30*, 8018−8026.
57. Marky, L. A., Rentzeperis, D., Luneva, N. P., Cosman, M., Geacintov, N. E., and Kupke, D. W. (1996) Differential hydration thermodynamics of stereoisomeric DNA-benzo[*a*]pyrene adducts derived from diol epoxide enantiomers with different tumorigenic potentials, *J. Am. Chem. Soc. 118*, 3804−3810.
58. Holbrook, J. A., Capp, M. W., Saecker, R. M., and Record, M. T. (1999) Enthalpy and heat capacity changes for formation of an oligomeric DNA duplex: Interpretation in terms of coupled processes of formation and association of single-stranded helices, *Biochemistry 38*, 8409−8422.
59. Mikulecky, P. J., and Feig, A. L. (2006) Heat capacity changes associated with nucleic acid folding, *Biopolymers 82*, 38- 58.
60. Breslauer, K. J., Freire, E., and Straume, M. (1992) Calorimetry: A tool for DNA and ligand-DNA studies, *Methods Enzymol. 211*, 533−567.
61. Petersen, M., Bondensgaard, K., Wengel, J., and Jacobsen, J. P. (2002) Locked nucleic acid (LNA) recognition of RNA: NMR solution structures of LNA:RNA hybrids, *J. Am. Chem. Soc. 124*, 5974−5982.
62. Nielsen, K. E., Rasmussen, J., Kumar, R., Wengel, J., Jacobsen, J. P., and Petersen, M. (2004) NMR studies of fully modified locked nucleic acid (LNA) hybrids: solution structure of an LNA:RNA hybrid and characterization of an LNA:DNA hybrid, *Bioconjugate Chem. 15*, 449−457.
63. Westhoff, E. (1988) Water: an integral part of nucleic acid structure, *Annu. Rev. Biophys. Biophys. Chem. 17*, 125−144.
64. Berman, H. M. (1991) Hydration of DNA, *Curr. Opin. Struct. Biol. 1*, 423−427.
65. Berman, H. M. (1994) Hydration of DNA, take 2, *Curr. Opin. Struct. Biol. 4*, 345−350.
66. Kankia, B. I., and Marky, L. A. (1999) DNA, RNA and DNA/RNA oligomer duplexes: A comparative study of their stability, heat, hydration and Mg2+ binding properties, *J. Phys. Chem. B 103*, 8759−8767.
67. Kankia, B. I., Kupke, D. W., and Marky, L. A. (2001) The incorporation of a platinated cross-link into duplex DNA yields an uptake of structural water, *J. Phys. Chem. B 105*, 11402−11405.
68. Feig, M., and Pettitt, B. M. (1998) A molecular simulation picture of DNA hydration around A- and B-DNA, *Biopolymers 48*, 199−209.
69. Drew, H. R., Wing, R. M., Takano, T., Broka, C., Tanaka, S., Itakura, K., and Dickerson, R. E. (1981) Structure of a B-DNA dodecamer: conformation and dynamics, *Proc. Natl. Acad. Sci. U.S.A. 78*, 2179−2183.
70. Kennard, O., Cruse, W. B., Nachman, J., Prange, T., Shakked, Z., and Rabinovich, D. (1986) Ordered water structure in an A-DNA octamer at 1.7 Å resolution, *J. Biomol. Struct. Dyn. 3*, 623−647.
71. Conner, B. N., Yoon, C., Dickerson, J. L., and Dickerson, R. E. (1984) Helix geometry and hydration in an A-DNA tetramer: IC-C-G-G, *J. Mol. Biol. 174*, 663−695.
72. Saenger, W., Hunter, W. N., and Kennard, O. (1986) DNA conformation is determined by economics in the hydration of phosphate groups, *Nature 324*, 385−388.
73. Egli, M., Portmann, S., and Usman, N. (1996) RNA hydration: a detailed look, *Biochemistry 35*, 8489−8494.


BI700996Z